



Influence of 2,5-bis(4-dimethylaminophenyl)-1,3,4-thiadiazole on corrosion inhibition of mild steel in acidic media

F. BENTISS¹, M. TRAISNEL² and M. LAGRENEE^{1*}

¹Laboratoire de Cristallochimie et Physicochimie du Solide, CNRS UPRESA 8012, ENSCL, BP. 108, F-59652 Villeneuve d'Ascq Cedex, France

²Laboratoire de Génie des Procédés d'Interactions Fluides Réactifs-Matériaux, UPRES EA 2698, ENSCL, BP. 108, F-59652 Villeneuve d'Ascq Cedex, France

(*author for correspondence, e-mail: michel.lagreneee@ensc-lille.fr)

Received 16 March 2000; accepted in revised form 5 July 2000

Key words: acidic media, adsorption, corrosion inhibition, mild steel, thiadiazole

Abstract

An example of a new class of corrosion inhibitors, namely, 2,5-bis(4-dimethylaminophenyl)-1,3,4-thiadiazole (DAPT) was synthesized and its inhibiting action on the corrosion of mild steel in 1 M HCl and 0.5 M H₂SO₄ at 30 °C was investigated by various corrosion monitoring techniques. A preliminary screening of the inhibition efficiency was carried out using weight loss measurements. At constant acid concentration, inhibitor efficiency increases with concentration of DAPT and is found to be more efficient in 0.5 M H₂SO₄ than in 1 M HCl. Potentiostatic polarization studies showed that DAPT is a mixed-type inhibitor. The effect of temperature on the corrosion behaviour of mild steel in 1 M HCl with addition of DAPT was studied in the temperature range from 25 to 60 °C. It was shown that adsorption is consistent with the Langmuir isotherm for 30 °C. The negative free energy of adsorption in the presence of DAPT suggests chemisorption of thiadiazole molecules on the steel surface.

1. Introduction

It has been observed that the adsorption of corrosion inhibitors depends mainly on certain physico-chemical properties of the molecule such as functional groups, steric factors, aromaticity, electron density at the donor atoms and π orbital character of donating electrons [1–5], and also on the electronic structure of the molecules [6, 7]. The title compound, abbreviated as DAPT, is an example of a new class of corrosion inhibitors, namely the 2,5-disubstituted 1,3,4-thiadiazoles. The aim of the present work is to investigate the efficiency of DAPT as corrosion inhibitor of mild steel in 1 M hydrochloric and 0.5 M sulfuric acid, in order to study the influence of a sulfur atom in the central part of the molecule. Thus, the effect of concentration and temperature of the inhibitor on inhibition properties was studied. The mode of adsorption and the corrosion inhibition mechanism on steel in acidic solutions are also discussed.

2. Experimental details

The tested inhibitor, namely 2,5-bis(4-dimethylaminophenyl)-1,3,4-thiadiazole (DAPT) was synthesised according to a previously described procedure [8]. The molecular formula of DAPT is shown in Figure 1. The

concentration range of inhibitor employed was varied from 0.25×10^{-4} to 5×10^{-4} M. Corrosion tests were performed on a mild steel of the following percentage composition: 0.09% P, 0.38% Si, 0.01% Al, 0.05% Mn, 0.21% C, 0.05% S and the remainder iron. For the gravimetric and electrochemical measurements, pre-treatment of the surface of specimens was carried out by grinding with emery paper of 600–1200 grit, rinsing with bidistilled water, ultrasonic degreasing in ethanol, and drying at room temperature before use. Solutions of 1 M HCl and 0.5 M H₂SO₄, were prepared by dilution of analytical grade 37% HCl and 96% H₂SO₄ with bidistilled water, respectively.

Gravimetric experiments were carried out in a double glass cell equipped with a thermostated cooling condenser. The solution volume was 100 ml. The steel specimens used had a rectangular form (length 2 cm, width 1 cm, thickness 0.06 cm). The maximum duration of tests was 24 h at 30 °C in non-deaerated solutions. At the end of the tests the specimens were carefully washed in ethanol under ultrasound and then weighed. Duplicate experiments were performed in each case and the mean value of the weight loss is reported. Weight loss allowed calculation of the mean corrosion rate in $\text{mg cm}^{-2} \text{h}^{-1}$.

Micrographs of the corroded and corrosion inhibited mild steel surface, coated by a film of 50 nm of gold by

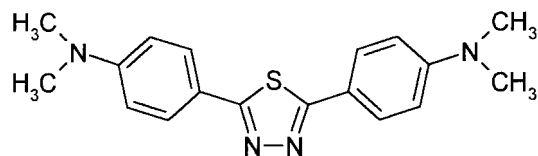


Fig. 1. Chemical formula of the DAPT.

sputtering, was taken using scanning electron microscopy (JEOL 5300). The energy of the acceleration beam employed was 20 kV.

Electrochemical measurements were carried out by means of impedance equipment (Tacussel-Radiometer PGZ 301) and controlled with Tacussel corrosion analysis software (Voltmaster 4).

Polarization experiments were carried out in a conventional three-electrode glass cell with a platinum counter electrode and a saturated calomel electrode (SCE) as reference with a Luggin capillary bridge. All tests were performed in deaerated solutions under continuously stirred conditions at room temperature. The procedure adopted for the polarization measurements was the same as described elsewhere [9]. For a given potential, the current was usually steady within 30 min. The cathodic branch was always determined first; the open-circuit potential was then reestablished and the anodic branch determined. The anodic and cathodic polarization curves were recorded by a constant sweep rate of 0.5 mV s^{-1} . Inhibition efficiencies were determined from corrosion currents calculated by the Tafel extrapolation method and fitting the curve to the polarization equation.

Impedance spectra were obtained in the frequency range 100 kHz to 10 mHz with ten points per decade at the corrosion potential after 24 h of immersion. A sine wave with 10 mV amplitude was used to perturb the system. Tests were performed in a polymethyl methacrylate (PMMA) cell with a capacity of 1000 ml. A saturated calomel electrode (SCE) was used as reference and a Pt plate was used as counter electrode. All potentials are reported vs SCE. All tests were performed at 30°C in non-deaerated solutions under unstirred conditions. Square sheets of mild steel of size ($5 \text{ cm} \times 5 \text{ cm} \times 0.06 \text{ cm}$), with exposed area 7.55 cm^2 , were used as the working electrode.

3. Experimental results and discussion

3.1. Gravimetric measurements

Tables 1 and 2 show the results for mild steel in 1 M HCl and 0.5 M H_2SO_4 at 30°C both in the absence and presence of DAPT. In most cases the inhibiting efficiency was greater than 95% and the corrosion rate was acceptable. The percentage inhibition efficiency E was calculated as described previously [10]. DAPT inhibited the corrosion of mild steel in both acids. As corrosion rate decreased, inhibition efficiency increased with

Table 1. Inhibition efficiency for various concentrations of DAPT for the corrosion of mild steel in 1 M HCl obtained from weight loss measurements at 30°C

| Inhibitor conc. / 10^{-4} M | Corrosion rate / $\text{mg cm}^{-2} \text{ h}^{-1}$ | Inhibition efficiency, E / % |
|---------------------------------------|---|--------------------------------|
| Blank | 2.021 | – |
| 0.25 | 0.289 | 85.7 |
| 0.5 | 0.096 | 95.2 |
| 1 | 0.056 | 97.2 |
| 2.5 | 0.042 | 97.9 |
| 5 | 0.037 | 98.1 |

Table 2. Inhibition efficiency for various concentrations of DAPT for the corrosion of mild steel in 0.5 M H_2SO_4 obtained from weight loss measurements at 30°C

| Inhibitor conc. / 10^{-4} M | Corrosion rate / $\text{mg cm}^{-2} \text{ h}^{-1}$ | Inhibition efficiency, E / % |
|---------------------------------------|---|--------------------------------|
| Blank | 6.346 | – |
| 0.25 | 0.581 | 90.8 |
| 0.5 | 0.360 | 94.3 |
| 1 | 0.208 | 96.7 |
| 2.5 | 0.106 | 98.3 |
| 5 | 0.037 | 99.4 |

increasing DAPT concentration in the test solution. The presence of DAPT gave high inhibiting efficiencies on the mild steel in 0.5 M H_2SO_4 and somewhat lower efficiency in 1 M HCl. This is probably due to the lesser surface coverage in HCl solutions.

To establish whether inhibition is due to the formation of an organic film on the metal surface, scanning electron micrographs were taken (Figures 2 and 3). Parallel features on the polished steel surface before exposure to the corrosive solution, which are associated with polishing scratches were observed (Figure 2). Examination of Figure 3 revealed that the specimen immersed in 1 M HCl containing DAPT was covered with a film, which inhibits corrosion (Figure 3). The

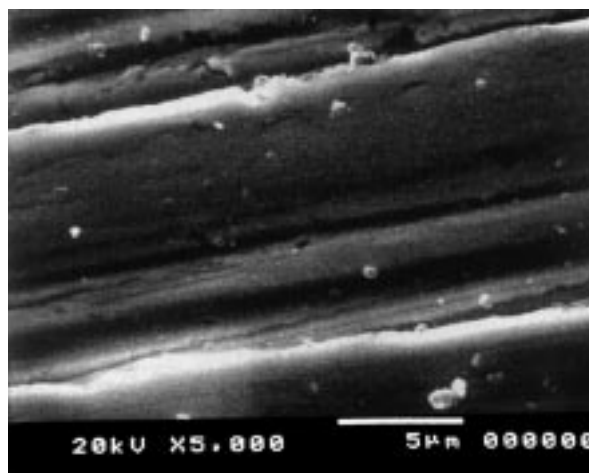


Fig. 2. SEM micrograph of polished surface for mild steel before its exposure to electrolyte.

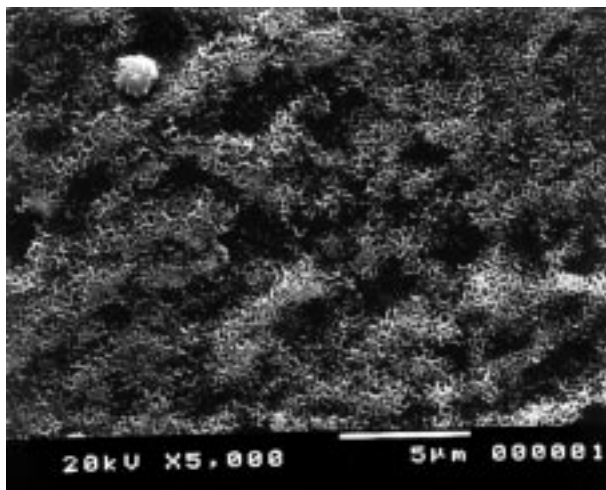


Fig. 3. SEM micrograph of the surface for mild steel after 24 h of immersion at 30 °C in 1 M HCl containing 10^{-4} M of DPAT.

protection provided by DAPT to mild steel in acidic solutions was retained when specimens dipped in acids containing the organic molecules were transferred into fresh acid without inhibitor. DAPT has a strong tendency to adhere to the steel surface. The DAPT molecules adsorb on the metal surface through sharing electrons between nitrogen or sulfur and iron atoms. This shows that the inhibition is due to the formation of a film of organic molecules on the metal surface (Figure 3).

3.2. Potentiostatic polarization study

Figures 4 and 5 show polarization curves for mild steel in 1 M HCl and 0.5 M H_2SO_4 with and without various concentrations of DAPT. DAPT suppressed the cathodic and anodic reactions. It is clear that the addition of DAPT hindered the acid attack on the steel electrode and a comparison of curves in both cases, showed that, with respect to the blank, increasing the concentration of the inhibitor gave rise to a consistent decrease in anodic and cathodic current densities indicating that DAPT acts as a mixed type inhibitor [11]. Calculated

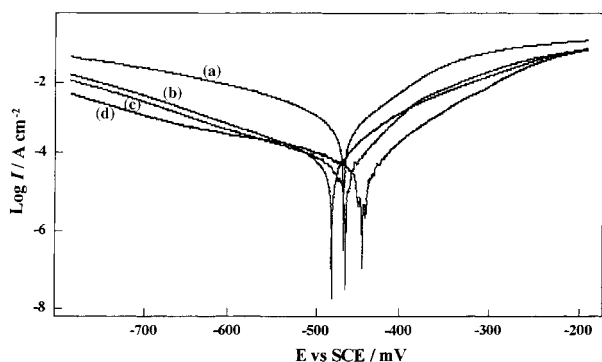


Fig. 4. Polarization curves of mild steel recorded in 1 M HCl containing different concentrations of DAPT. Key: (a) blank, (b) 0.25×10^{-4} M, (c) 0.5×10^{-4} M and (d) 1×10^{-4} M.

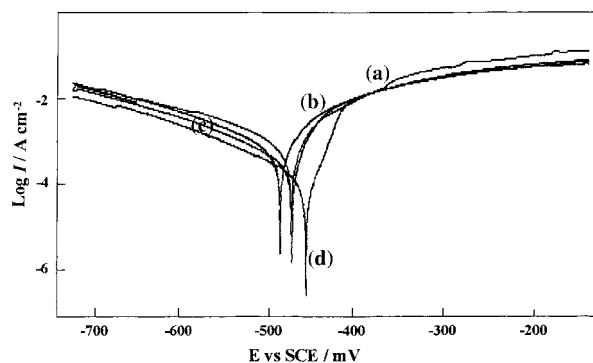


Fig. 5. Polarization curves of mild steel recorded in 1 M HCl containing different concentrations of DAPT. Key: (a) blank, (b) 0.25×10^{-4} M, (c) 0.5×10^{-4} M and (d) 1×10^{-4} M.

polarization results, that is, corrosion potential (E_{corr}) and corrosion current density (I_{corr}) obtained by extrapolation of the Tafel lines are listed in Tables 3 and 4. The calculated percentage inhibition efficiencies (E) of DAPT are also given. Analysis of these data shows that I_{corr} decreased with addition of DAPT in 1 M HCl and 0.5 M H_2SO_4 , due to increase in the blocked fraction of the electrode surface by adsorption.

3.3. AC impedance study

The results described below can be interpreted in terms of the equivalent circuit of the electrical double layer shown in Figure 6, which has been used previously to model the iron–acid interface [12]. Figure 7 shows Bode plots for uninhibited steel in 1 M HCl and for steel in 1 M HCl containing 10^{-4} M of DAPT. It can be seen that the addition of 10^{-4} M DAPT decreases the low frequency value of the impedance, that is, ($R_t + R_s \approx R_t$) by a factor of nearly 30. The high frequency value on the bode plot is R_s . As can be seen from the impedance

Table 3. Electrochemical parameters for the corrosion of mild steel in 1 M HCl containing different concentrations of DAPT at 30 °C and the corresponding corrosion efficiency

| Inhibitor conc. / 10^{-4} M | E_{corr} vs SCE / mV | I_{corr} / $\mu\text{A cm}^{-2}$ | E / % |
|-------------------------------|-------------------------------|---|---------|
| Blank | -470 | 570 | – |
| 0.25 | -481 | 61 | 89.3 |
| 0.5 | -467 | 55 | 90.3 |
| 1 | -446 | 35 | 93.9 |

Table 4. Electrochemical parameters for the corrosion of mild steel in 0.5 M H_2SO_4 containing different concentrations of DAPT at 30 °C and the corresponding corrosion efficiency

| Inhibitor conc. / 10^{-4} M | E_{corr} vs SCE / mV | I_{corr} / $\mu\text{A cm}^{-2}$ | E / % |
|-------------------------------|-------------------------------|---|---------|
| Blank | -482 | 1540 | – |
| 0.25 | -490 | 133 | 91.4 |
| 0.5 | -476 | 119 | 92.3 |
| 1 | -460 | 75 | 95.1 |

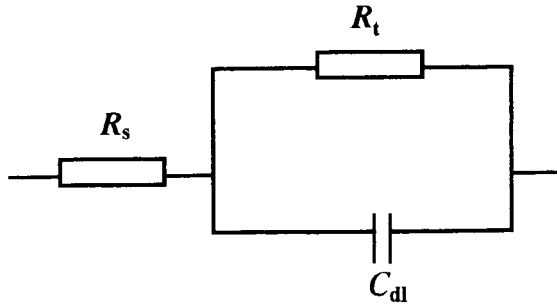


Fig. 6. Equivalent circuit for the metal–acid interface.

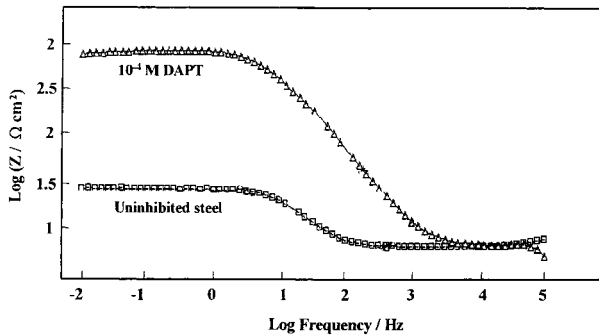


Fig. 7. Bode plots for mild steel in 1 M HCl.

results shown in Figure 7, the increase in polarization resistance in the presence of DAPT (compared to inhibitor-free solution) is related to the corrosion protection effect of the molecule.

Figures 8 and 9 show the corresponding Cole–Cole plots [13] (usually called Nyquist plots) for mild steel in both acids at various concentrations of DAPT. The best semicircle can be fitted through the data points in the Nyquist plot using a nonlinear least square fit so as to give the intersections with the x axis, which are R_s and $(R_s + R_t)$ [14]. Double-layer capacitance values (C_{dl}) were calculated from the Nyquist plots as described elsewhere [15]. It is apparent from these plots that the impedance response of mild steel in uninhibited HCl and H_2SO_4 solutions has significantly changed after the addition of DAPT. This indicates that the impedance of inhibited substrate increases with increasing inhibitor concentration in both acids. The corrosion kinetic parameters derived from the Nyquist plots and percentage inhibition efficiency (E) are given in Tables 5 and 6. The greatest effect was observed at 10^{-3} M of DAPT which produced R_t values of $1133 \Omega \text{ cm}^2$ in 1 M HCl

Table 5. Impedance measurements and inhibition efficiency for mild steel in 1 M HCl containing different concentrations of DAPT at 30 °C

| Inhibitor conc. / 10^{-4} M | R_t / $\Omega \text{ cm}^2$ | E_{rest} potential vs SCE / mV | C_{dl} / $\mu\text{F cm}^{-2}$ | E / % |
|-------------------------------|-------------------------------|----------------------------------|----------------------------------|---------|
| Blank | 20 | -478 | 785 | – |
| 0.25 | 564 | -473 | 42 | 96.4 |
| 0.5 | 893 | -445 | 39 | 97.7 |
| 1 | 939 | -444 | 36 | 97.8 |
| 2.5 | 1017 | -451 | 28 | 98.0 |
| 5 | 1133 | -455 | 22 | 98.2 |

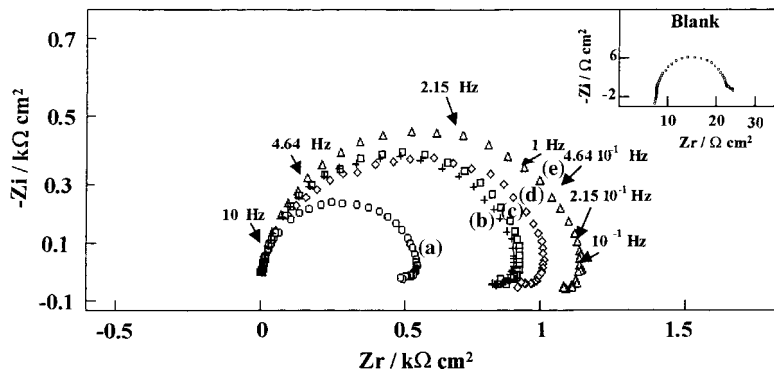


Fig. 8. Nyquist diagrams for mild steel in 1 M HCl containing different concentrations of DAPT. Key: (a) 0.25×10^{-4} M, (b) 0.5×10^{-4} M, (c) 1×10^{-4} M, (d) 2.5×10^{-4} M and (e) 5×10^{-4} M.

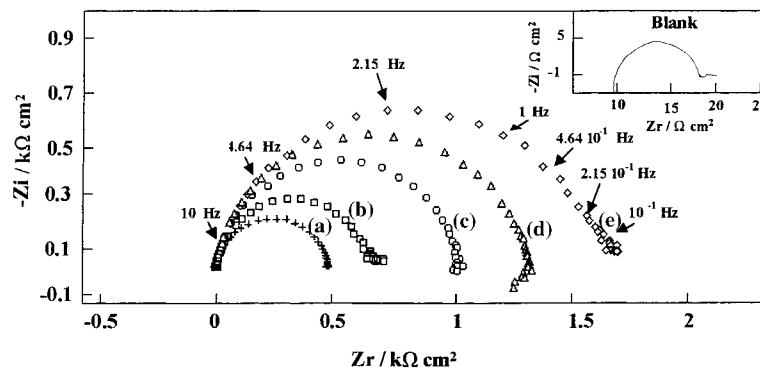


Fig. 9. Nyquist diagrams for mild steel in 0.5 M H_2SO_4 containing different concentrations of DAPT. Key: as for Figure 8.

Table 6. Impedance measurements and inhibition efficiency for mild steel in 0.5 M H₂SO₄ containing different concentrations of DAPT at 30 °C

| Inhibitor conc. /10 ⁻⁴ M | R _t /Ω cm ² | E _{rest} potential vs SCE /mV | C _{dl} /μF cm ⁻² | E /% |
|-------------------------------------|-----------------------------------|--|--------------------------------------|------|
| Blank | 9 | -470 | 1775 | – |
| 0.25 | 478 | -464 | 95 | 98.1 |
| 0.5 | 652 | -463 | 61 | 98.6 |
| 1 | 1017 | -454 | 49 | 99.1 |
| 2.5 | 1311 | -425 | 39 | 99.3 |
| 5 | 1642 | -441 | 30 | 99.6 |

and 1642.2 Ω cm² in 0.5 M H₂SO₄ (Tables 5 and 6). When the concentration of inhibitor increases, C_{dl} values decrease. Decrease in the C_{dl}, which can result from a decrease in local dielectric constant and/or an increase in the thickness of the electrical double layer, suggests that the DAPT molecules function by adsorption at the metal–solution interface [16]. Similar behaviour is observed in both media. In the case of impedance studies, the percentage inhibition efficiency (E) is calculated by charge transfer resistance as described elsewhere [15]. Inhibition efficiency increases with inhibitor concentration reaching a maximum value at 5 × 10⁻⁴ M in both acids. But inhibition efficiency is found to be greater in H₂SO₄ solutions. This may be due to the availability of more sites on the metal surface in H₂SO₄ solution because of the lesser adsorption of the sulfate ions on the steel surface [17]. The a.c. impedance study also confirms the inhibiting character of DAPT obtained with polarization curves and weight loss measurements in both acid solutions.

3.4. Effect of temperature

The effect of temperature on inhibition efficiency was determined in 1 M HCl containing 0.5 × 10⁻⁴ M of DPAT at temperatures of 25, 30, 40, 50 and 60 °C using potentiodynamic polarization curves. The results are given in Figures 10 and 11. Corresponding data are given in Tables 7 and 8. As expected, the corrosion current density increased by 1 order of magnitude with increasing temperature both in uninhibited and inhi-

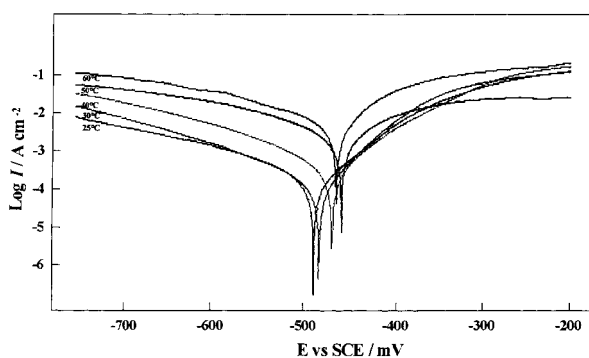


Fig. 10. Effect of temperature on the cathodic and anodic responses for mild steel in deaerated 1 M HCl.

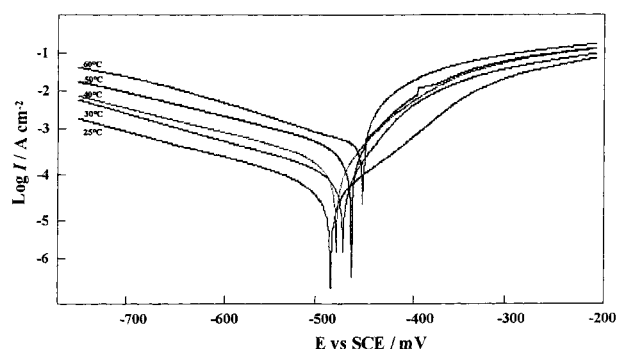


Fig. 11. Effect of temperature on the cathodic and anodic responses for mild steel in deaerated 1 M HCl + 0.5 × 10⁻⁴ M of DPAT.

Table 7. The influence of temperature on the electrochemical parameters for mild steel electrode immersed in 1 M HCl

| Temperature /°C | E _{corr} vs SCE /mV | I _{corr} /μA cm ⁻² |
|-----------------|------------------------------|--|
| 25 | -480 | 398 |
| 30 | -470 | 570 |
| 40 | -460 | 957 |
| 50 | -450 | 1626 |
| 60 | -455 | 3506 |

Table 8. The influence of temperature on the electrochemical parameters for mild steel electrode immersed in 1 M HCl + 0.5 × 10⁻⁴ M of DPAT

| Temperature /°C | E _{corr} vs SCE /mV | I _{corr} /μA cm ⁻² | E /% |
|-----------------|------------------------------|--|------|
| 25 | -482 | 42 | 89.4 |
| 30 | -467 | 55 | 90.3 |
| 40 | -476 | 105 | 89.0 |
| 50 | -461 | 184 | 88.7 |
| 60 | -448 | 391 | 88.8 |

bited solutions, and the values of inhibition efficiency of DAPT were nearly constant in the temperature range (Tables 7 and 8).

Corrosion current density for steel increased more rapidly with temperature in the absence of inhibitor (blank). These result confirmed that DAPT acts as an efficient inhibitor in the range of temperature studied. The DAPT inhibitor efficiency was temperature-independent. The corrosion reaction can be regarded as an Arrhenius-type process, the rate of which is given by

$$I_{\text{corr}} = k \exp\left(-\frac{E_a}{RT}\right) \quad (1)$$

where I_{corr} is the corrosion current density, E_a is the apparent activation corrosion energy, T is the absolute temperature, k is the Arrhenius preexponential constant and R is the universal gas constant. This equation can be used to calculate the E_a values of the corrosion reaction without and with 0.5 × 10⁻⁴ M of DPAT. Plotting the natural logarithm of the corrosion current density against 1/T, the activation energy can be calculated

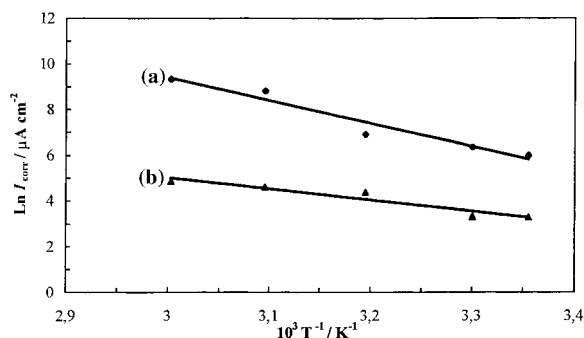
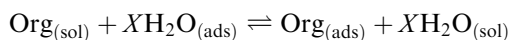


Fig. 12. Arrhenius slopes calculated from corrosion current density for mild steel in: (a) 1 M HCl and (b) 1 M HCl + 0.5×10^{-4} M of DPAT.

from the slope. Arrhenius plots for the corrosion current density of mild steel are given in Figure 12. The calculated values of the apparent activation corrosion energy in the absence and presence of DPAT are 84 kJ mol^{-1} and 41 kJ mol^{-1} , respectively. The reduction in the activation energy in the presence of DPAT may be attributed to the chemisorption of DPAT inhibitor on steel [18, 19]. Therefore, we can assume that the film formation observed by SEM occurs through the process of adsorption of the organic molecules on steel surface.

3.5. Adsorption isotherm

The values of surface coverage, Θ , corresponding to different concentrations of DPAT at 30°C have been used to explain the best isotherm to determine the adsorption process. The adsorption of an organic adsorbate at a metal–solution interface can be represented as substitutional adsorption process between the organic molecules in the aqueous solution $\text{Org}_{(\text{sol})}$ and the water molecules on the metallic surface $\text{H}_2\text{O}_{(\text{ads})}$ [20]:



where $\text{Org}_{(\text{sol})}$ and $\text{Org}_{(\text{ads})}$ are the organic molecules in the aqueous solution and adsorbed on the metallic surface, respectively, $\text{H}_2\text{O}_{(\text{ads})}$ is the water molecules on the metallic surface, X is the size ratio representing the number of water molecules replaced by one molecule of organic adsorbate.

The degree of surface coverage, Θ , for different concentrations of DPAT was expressed by the ratio $E\%/100$. Attempts were made to fit Θ values to various isotherms including Frumkin, Langmuir and Temkin. By far the best fit was obtained with the Langmuir isotherm. This Langmuir model has been used for other inhibitor systems [21]. According to this isotherm Θ is related to concentration inhibitor C_{inh} via

$$\frac{\Theta}{\Theta - 1} = kC_{\text{inh}} \exp\left(\frac{-\Delta G_{\text{ads}}^\circ}{RT}\right) \quad (2)$$

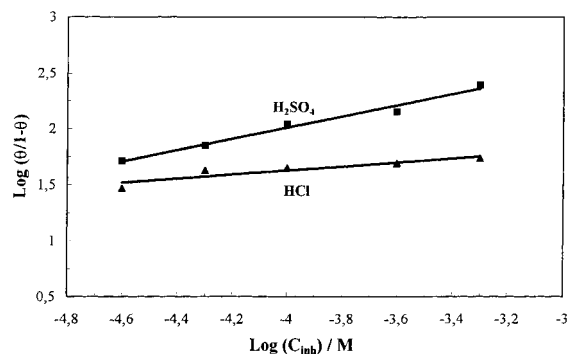


Fig. 13. Langmuir isotherm adsorption model of DPAT on the steel surface in $0.5 \text{ M H}_2\text{SO}_4$ from impedance measurements.

This equation predicts a linear plot between values of $\log(\Theta/1 - \Theta)$ and $\log C_{\text{inh}}$ (Figure 13); $\Delta G_{\text{ads}}^\circ$ is the free energy of adsorption and k is a constant [22].

The strong correlation ($r = 0.92$ in 1 M HCl and $r = 0.99$ in $0.5 \text{ M H}_2\text{SO}_4$) for the Langmuir adsorption isotherm plot for DPAT at 30°C confirms the validity of this approach. The values of the free energy of adsorption as calculated from the Langmuir-type adsorption isotherm in 1 M HCl and $0.5 \text{ M H}_2\text{SO}_4$ were $-39.3 \text{ kJ mol}^{-1}$ and $-43.1 \text{ kJ mol}^{-1}$, respectively. The largest negative value of $\Delta G_{\text{ads}}^\circ$ in the case of $0.5 \text{ M H}_2\text{SO}_4$ indicates that DPAT is strongly adsorbed on the steel surface [23].

From this finding, we can say that DPAT is adsorbed on mild steel. As far as the inhibition process is concerned, it is generally assumed that the adsorption of the inhibitor at the metal–solution interface is the first step in the action mechanism of inhibitors in aggressive acid media. Four types of adsorption may take place involving organic molecules at the metal–solution interface: (i) electrostatic attraction between charged molecules and the charged metal, (ii) interaction of unshared electron pairs in the molecule with the metal, (iii) interaction of π -electrons with the metal and (iv) a combination of the above [24].

Chemisorption involves charge sharing or charge transfer from the inhibitor molecules to the surface to form a coordinate-type bond. In fact, electron transfer is typical for transition metals having vacant, low-energy electron orbitals. Electron transfer can be expected with compounds having relatively loosely bound electrons [25]. Inhibition efficiency depends on several factors, such as the number of adsorption sites and their charge density, molecular size, heat of hydrogenation, mode of interaction with the metal surface and the formation metallic complexes [26]. Most organic inhibitors contain at least one polar group with an atom of nitrogen, sulphur or oxygen; each of them might be a chemisorption centre. The inhibitive properties of such compounds depends on the electron densities around the chemisorption centre; the higher the electron density at the centre, the more effect is inhibitor.

The following explanations are postulated: DPAT interferes in the dissolution reaction by adsorption at

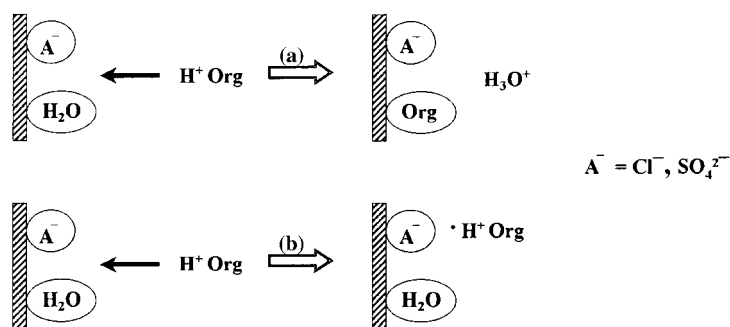


Fig. 14. Schematic representations of (a) competitive, and (b) cooperative adsorption of thiadiazole-type organic compound in acid solutions.

the metal surface in two different ways. First, the inhibitor competes with Cl^- or SO_4^{2-} ions for sites at the water covered anodic surface. In doing so, the protonated inhibitor loses its associated proton(s) in entering the double layer and chemisorbs by donating electrons to the metal. In addition, the protonated inhibitor electrostatically adsorbs onto the anion covered surface, through its cationic form. Both modes of adsorption are depicted in Figure 14. DAPT thus plays a dynamic role at the interface and interferes with dissolution reaction by participating in a number of adsorption–desorption steps, rather than solely by a blockage of sites [27–29]. Iron sites covered by adsorbed inhibitor molecules (competitive or cooperative adsorption) are dissolution precursors. As chloride ions are more strongly adsorbed on the iron surface than sulfate ions, the cationic form of the DAPT molecule can jointly adsorb on the metal surface without much difficulty in HCl compared with H_2SO_4 [11]. However, the inhibition efficiency obtained by DAPT was found to be higher in H_2SO_4 solutions. This may be due to the availability of more sites on the metal surface in H_2SO_4 solution because of the lesser adsorption of the sulfate ions on the steel surface. In H_2SO_4 , adsorption through the lone pairs of heteroatoms and π -electrons of the DAPT molecule outweighs the adsorption due the cationic form of the DAPT molecule on the metal surface. This is probably due to the shape of the sulfur orbitals of the heterocyclic compound.

4. Conclusion

DAPT inhibits the corrosion of mild steel in both acids, but the better performance is seen in the case of H_2SO_4 . SEM reveals the formation of a smooth, dense protective layer in the presence of an effective inhibitor blend. The adsorbed inhibitor molecules are assumed to retard corrosion by reducing the number of available surface sites for corrosion and also by slowing the rate of the corrosion reactions. DAPT is found to affect both the cathodic and anodic processes; that is, the inhibitor is of mixed type. The concentration dependence of the inhibition efficiency calculated from weight loss measurements and electrochemical studies has the same

tendency. The inhibition efficiency of DAPT is temperature-independent and its addition leads to a decrease in activation corrosion energy. Adsorption of DAPT on the steel surface from 1 M HCl and 0.5 M H_2SO_4 follows the Langmuir isotherm, indicating that the main inhibition process occurs via adsorption. The negative value of ΔG_A° obtained from this study indicates that DAPT was strongly adsorbed on the steel surface.

References

1. E. Khamis, *Corrosion* **46** (1990) 476.
2. E. Stupnisek-Lisac and S. Podbrscek, *J. Appl. Electrochem.* **24** (1994) 779.
3. G. Schmitt and K. Bedbur, *Werkst. Korros.* **36** (1985) 273.
4. I.L. Rosenfeld, 'Corrosion Inhibitors' (McGraw-Hill, New York, 1981).
5. E. Stupnisek-Lisac and M. Metikos-Hukovic, *Br. Corros. J.* **28** (1993) 74.
6. S.L. Granese, B.M. Rosales, C. Oviedo and J.O. Zerbino, *Corros. Sci.* **33** (1992) 1439.
7. S.L. Granese, *Corrosion* **44** (1988) 322.
8. G. Mazzone, G. Puglisi, F. Bonina and A. Corsaro, *J. Heterocyclic Chem.* **20** (1983) 1399.
9. F. Bentiss, M. Lagrenee, M. Traisnel and J.C. Hornez, *Corrosion* **55** (1999) 968.
10. F. Bentiss, M. Lagrenee, M. Traisnel, B. Mernari and H. Elattari, *J. Appl. Electrochem.* **29** (1999) 1073.
11. S. Muralidharan, K.L.N. Phani, S. Pitchumani, S. Ravichandran and S.V.K. Iyer, *J. Electrochem. Soc.* **142** (1995) 1478.
12. F. Mansfeld, *Corrosion* **36** (1981) 301.
13. K.S. Cole and R.H. Cole, *J. Chem. Phys.* **9** (1941) 341.
14. E. McCafferty, V. Pravdic and A.C. Zettlemyer, *Trans. Faraday Soc.* **66** (1970) 1720.
15. F. Bentiss, M. Traisnel, L. Gengembre and M. Lagrenee, *Appl. Surf. Sci.* **237** (1999) 152.
16. E. McCafferty and N. Hackerman, *J. Electrochem. Soc.* **119** (1972) 146.
17. W.J. Lorenz and F. Mansfeld, *Corros. Sci.* **21** (1981) 647.
18. T. Szauer and A. Brand, *Electrochim. Acta* **26** (1981) 1219.
19. S. Sankarapavinasam, F. Pushpanaden and M. Ahmed, *Corros. Sci.* **32** (1991) 193.
20. G. Moretti, G. Quartarone, A. Tassan and A. Zingales, *Werkst. Korros.* **45** (1994) 641.
21. A.M.S. Abdel and A. El. Saied, *Trans. SAEST* **16** (1981) 197.
22. S. Kertit and B. Hammouti, *Appl. Surf. Sci.* **93** (1996) 59.
23. J.D. Talati and D.K. Gandhi, *Corros. Sci.* **23** (1983) 1315.
24. D. Schweinsberg, G. George, A. Nanayakkara and D. Steiner, *Corros. Sci.* **28** (1988) 33.
25. F. Mansfeld, 'Corrosion Inhibitors' (Marcel Dekker, New York, 1987), p. 119.

26. A. Fouda, M. Moussa, F. Taha and El Neanaa, *Corros. Sci.* **26** (1986) 719.
27. N. Hackerman and E. McCafferty, Proceedings of the 5th International Congress on 'Metallic Corrosion' (Tokyo, 1972), p. 542.
28. N. Hackerman, E. Snavely, Jr and J.S. Payne, Jr, *J. Electrochem. Soc.* **113** (1966) 677.
29. T. Murakawa and N. Hackerman, *Corros. Sci.* **4** (1964) 387.